

EFFICIENT TOPOGRAPHIC DEGRADATION ON CERES AS REVEALED BY THE EQUILIBRIUM POPULATION OF SMALL CRATERS. M. Hirabayashi¹, C. I. Fassett², P. Montalvo¹, H. C. J. Cheng³, C. Klimczak³, ¹Auburn University, Auburn, AL, ²NASA Marshall Space Flight Center, Huntsville, AL, ³University of Georgia, Athens, GA.

Introduction: Ceres exhibits its heavily cratered surface. While some craters look fresh, other craters are highly degraded [e.g., 1-2]. Like on other airless bodies, the various crater degradation levels observed imply ongoing surface evolution driven by two competing mechanisms: impacts forming new craters, and degradation of old craters [3]. This study uses a statistical approach to characterize the degradation efficiency, i.e., how efficiently craters are destroyed given new crater production. We show that Ceres's impact-driven degradation erases craters smaller than 1 km in diameter more efficiently than an ideal geometric emplacement condition (cookie cutting), likely due to ejecta blanketing and topographic diffusion. We also compare the degradation efficiencies on Ceres with those on Vesta, Moon, and Mercury, showing faster degradation on Ceres than other bodies (except Vesta).

Crater equilibrium: When a planetary surface gets bombarded continuously, the visible crater number ceases to grow because new crater emplacements start degrading/removing old craters. Degraded craters become challenging to recognize; at some point, the crater erasure rate matches the crater formation rate. This condition, known as crater equilibrium (or crater saturation), exhibits unique crater population features, one of which is a distinctive size-frequency distribution from the crater production distribution. While there are many factors, such as crater production and resurfacing, that control the cumulative slope [3, 4], a typical crater equilibrium condition has a cumulative power law slope of about -2 for a steeper production slope [3-6]. One approach for quantifying the equilibrium phenomenon is to characterize how efficiently existing craters become invisible. While non-impact processes including active flows can also control crater equilibrium, we do not account for this effect.

Methods: The present approach statistically tracks the evolution of the crater population [6]. The idea is that the discrepancy between the crater equilibrium population and the crater production population is a function of degradation efficiency. To quantify this efficiency, the model defines a degradation parameter. This parameter specifies a ratio of an actual degradation number to an idealized degradation number defined by geometric emplacement (cookie cutting).

The degradation parameter is a function of crater diameter, denoted as $k(D)$, where D is the crater diameter. The higher the degradation efficiency, the higher the degradation parameter (i.e., a crater of size D becomes invisible more efficiently). By definition, because the unity value defines the geometric

emplacement condition, non-unity values mean a factor of efficiency. $k(D)$ strongly depends on the geological conditions and thus may be independently determined by incorporations of earlier works [5, 7].

The present model considers $k(D)$ unknown and determines it by comparing the observed crater distribution and crater production. There are two steps for this analysis. First, the model imports the observed cumulative crater population and determines a produced crater number using model chronology and production functions. Second, it assesses $k(D)$ using a Runge-Kutta scheme to solve a first-order ordinary differential equation that characterizes the balance in crater frequency between addition and removal.

Results: We consider the cratered surface populations of Haulani and Nawish on Ceres. We pick one location for each quadrangle and use one HAMO image and one LAMO image to count craters with sizes between 100 m and 100 km. We use a Lunar Based Model (LBM) and an Asteroid Based Model (ABM) [1] to determine the production functions (Figure 1). The detachment of the observed crater number from the production number seems to occur at ~4-5 km (LBM) and ~20 km (ABM) for both Haulani and Nawish. While there are other crater production models [10, 11], adapting the model to them will be our future work.

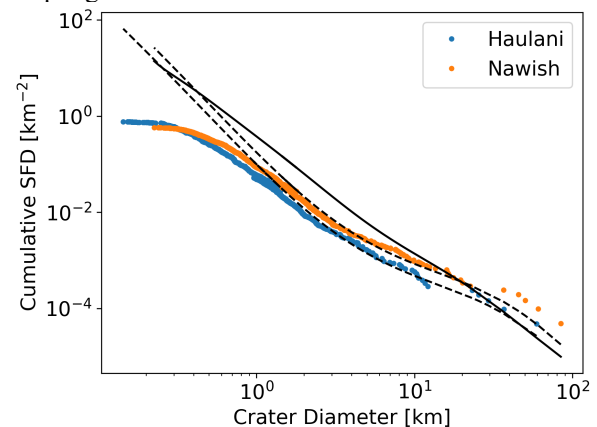


Figure 1. Cumulative Size-Frequency Distributions (CSFDs) of Haulani and Nawish on Ceres. The dashed lines give ABM, while the solid line shows LBM [1].

Figure 2 shows $k(D)$. In general, it increases as the diameter becomes small. This behavior with diameter is expected because the geomorphic work needed to erase the topography of small craters is less than at larger sizes, and the baseline cookie cutter model does not consider topography. For both Haulani and Nawish, the trends are similar; however, different production models change $k(D)$. LBM gives clear negative slopes

(red and orange), while ABM contributes to flat slopes (blue and green). This variation results from the equilibrium slopes relative to the production slope; the smaller the slope power difference, the flatter the degradation slope. $k(D) > 1$ happens when $D < 1-2$ km for LBM and $D < 10-15$ km for ABM, given both Haulani and Nawish. Thus, taking the lower bound, i.e., 1 km, concludes that craters at $D < 1$ km are degraded more efficiently than geometric emplacement due to ejecta blanketing and topographic diffusion.

Discussion: To infer how efficiently craters on Ceres have been removed, we compare crater regions that were reported to reach crater equilibrium on Ceres, Vesta, Mercury, and Moon [11-13]. Figure 3 illustrates all the equilibrium slopes (presumably the shallower parts) to be aligned approximately along the -2 slope. Importantly, this also supports that the two regions on Ceres are in crater equilibrium. Using provided production functions for Vesta, Mercury, and Moon [14-16], we compute $k(D)$ for each body (Figure 4). Note that because of the similarities of our Ceres test areas, we only show the Nawish region. The results show that regardless of the production models, Ceres gives higher $k(D)$ for large craters than Moon and Mercury. $k(D)$ for Vesta rapidly increases up to ~ 20 at $D < 3$ km, reaching the highest among the test bodies. The derived $k(D)$ s in these measurements lead to a spectrum of inferred efficiency: Vesta > Ceres > Mercury > Moon.

It may be reasonable that craters on Ceres have more efficiently been degraded than those on the Moon. Objects have been bombarded more violently in the main belt than around the Earth, giving higher impact fluxes (regardless of low impact velocities) [9]. Crater degradation on Mercury may also be relatively efficient because of its unique orbital condition [17] and the impactor speed. Vesta's relatively high $k(D)$, compared to Ceres's $k(D)$, can be explained by the fact that the selected crater count area is within Saturnalia Fossa, a tectonic landform, where mass movements over its sloping surface may effectively degrade craters [13].

In sum, degradation on Ceres is more efficient than on the Moon and Mercury, but less than on Vesta. As expected, sub-kilometer-sized craters have been removed more efficiently than geometrical emplacement.

Acknowledgments: M.H., C.I.F., and P.M. thank support from NNH19ZDA001N-DDAP.

References: [1] Hiesinger et al. (2016), Science 353 (6303), [2] Schmedemann et al. (2018), GRL, 43, 11,987–11,993, [3] Minton et al. (2015), Icarus 247, 172–190, [4] Richardson (2009), Icarus, 204(2), 697–715, [5] Minton et al. (2019), Icarus 326, 63–87, [6] Hirabayashi et al. (2017), Icarus 289, 134–143, [7] Fassett et al. (2017), GRL 44, 5326–5335, [8] Frigeri et al. (2018), Icarus 316, 114–127, [9] Bottke et al. (2020),

AJ, 160, 14, [10] Roig and Nesvorný (2020), AJ 160, 110, [11] Fassett et al. (2018), LPSC Abstract, 6129, [12] Gault (1970), Radio Science 5, 273–291, [13] Cheng et al. (2021), submitted to Icarus, [14] Le Feuvre and Wieczorek (2011), Icarus 214, 1–20, [15] Schmedemann et al. (2014), PSS 103, 104–130, [16] Hartmann et al. (2001), SSR 96 (1–4), 55–86, [17] Roig et al. (2016), ApJL 820, L30.

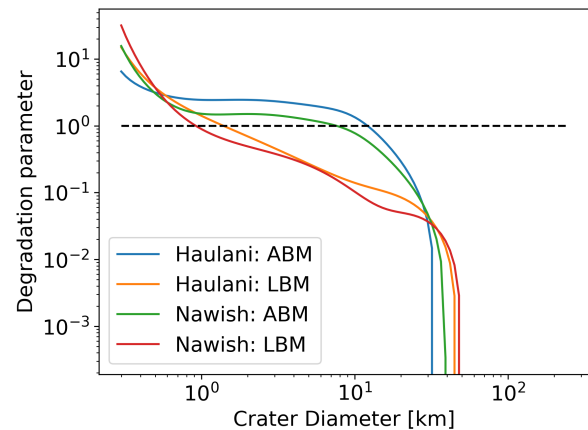


Figure 2. $k(D)$ of Haulani and Nawish on Ceres.

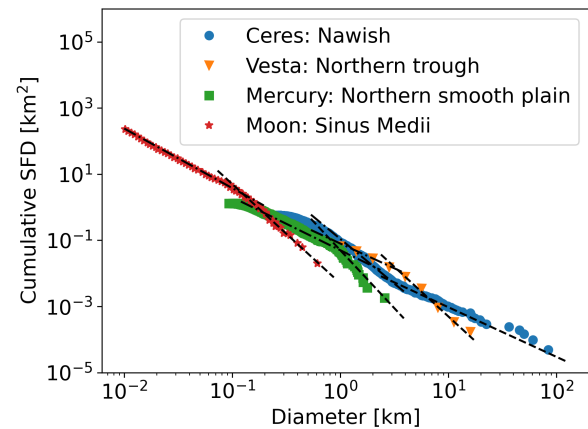


Figure 3. CSFDs of Ceres, Vesta, Mercury, and Moon. The dashed lines are the production function slopes, while the dot-dashed lines are the equilibrium slopes.

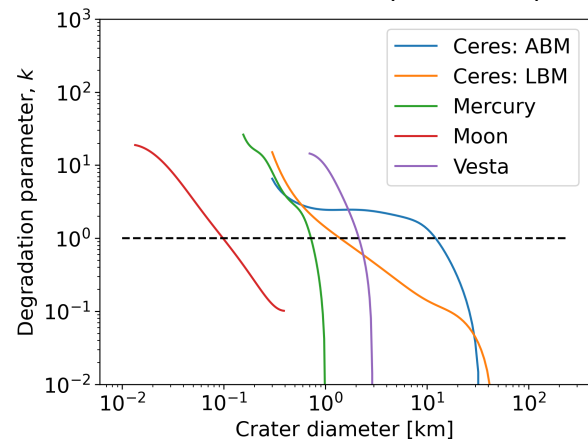


Figure 4. $k(D)$ of the selected regions on four bodies.